Fibers and Polymers (2023) 24:3761–3774
https://doi.org/10.1007/s12221-023-00360-z

Online ISSN 1875-0052
Print ISSN 1229-9197

REGULAR ARTICLE

Preparation and Characterization of Viburnum Opulus Containing Electrospun Membranes as Antibacterial Wound Dressing

Adile Yuruk[1] · Sevil Dincer Isoglu[1] · Ismail Alper Isoglu[1]

Received: 6 September 2022 / Revised: 28 November 2022 / Accepted: 1 December 2022 / Published online: 22 September 2023

Abstract

Herein, we fabricated polycaprolactone/gelatin electrospun membranes possessing different amounts of *Viburnum Opulus* extract (0, 25, 35, 50%, w/v) as an antibacterial wound dressing. We investigated chemical, morphological, physical, and mechanical properties as well as in vitro degradation behavior of the electrospun membranes. The antibacterial activities of membranes were evaluated against gram-positive *Staphylococcus aureus (S. aureus)* and gram-negative *Escherichia coli (E. coli)*. The membranes containing *Viburnum Opulus* exhibited excellent antibacterial activity with the formation of inhibition zones of 25 mm to 36 mm against *Escherichia coli* and 14 mm to 25 mm against *Staphylococcus aureus*. The fiber diameters rose from 591 to 1222 nm after adding *Viburnum Opulus* extract. The extract-containing membranes displayed superior swelling, cell viability, and proliferation properties to neat membranes. Our results showed that the polycaprolactone/gelatin electrospun membranes containing *Viburnum Opulus* could be a suitable material for wound dressing applications.

Keywords Electrospinning · Wound dressing · Antibacterial · Plant extract · Viburnum Opulus

1 Introduction

The skin is the largest organ in the body serving as an obstacle that protects tissues or organs from mechanical, chemical, and biological external factors, especially microbial pathogens [1]. Since the skin is directly in contact with these factors, it may be impaired and injured by some agents, such as physical, chemical, and thermal, or some diseases, including diabetes and surgery [2]. Every year, 8.2 million people suffer from acute and chronic skin wounds, and medical care costs ranged from $28.1 billion to $96.8 billion in 2014 [3, 4]. Wound healing has gained significant attention since millions of patients suffer from acute or chronic skin wounds. It is a complex process that aims to repair the anatomic structure and function of the skin [5, 6]. The wound healing process includes the inflammation/homeostasis phase, the proliferation phase, protein synthesis and wound contraction, and the remodeling phase, respectively [7]. However, the wound healing process may be restricted due to infection by microorganisms such as bacteria [8, 9]. That is why there is a massive need for a wound dressing material that has an antibacterial effect of preventing the growth of bacteria effectively and can accelerate the healing, mimic the skin and be safe for human use [10]. The traditional wound dressing materials cannot fulfill the clinical requirements for wound healing [2]. Electrospinning is a unique and effective technique to produce uniform fibers with diameters ranging from micro-meters to nano-meters [11, 12]. Although many fabricating fibrous matrices processes have already been known, the electrospinning technique is admired for its cost-efficiency, simplicity, and versatility [13, 14]. A wound dressing material must provide physical protection, prevent bacterial invasion, and allow wound exudate absorption and exchange of gas and fluids [15]. Therefore, the electrospun membranes gain considerable interest due to their large surface-area-to-volume ratio, high permeability for gas and fluids such as wound exudate, and suitable mechanical properties [11]. Besides, electrospun wound dressing membranes have many advantages over conventional materials, such as being adjustable pore structure, mimicking the ability to ECM, providing liquid and gas permeability, and keeping the wound area moist [16, 17]. In addition, due to their high surface area to volume ratio, electrospun membranes allow cell adhesion and proliferation and prevent fluid collection by absorbing the exudate fluid in the wound area [18].

✉ Ismail Alper Isoglu
alper.isoglu@agu.edu.tr

[1] Department of Bioengineering, Abdullah Gul University, Kocasinan, Kayseri 38080, Turkey

Poly(caprolactone) (PCL), polylactic acid, polyglycolic acid, poly-hydroxy acids, and their copolymers are well-known synthetic polymers for the production of wound dressing material using the electrospinning technique [2]. PCL, an FDA-approved biodegradable and biocompatible polyester with a semi-crystalline structure, is a highly preferred polymer for electrospinning because of the tailorable mechanical and structural properties, degradation kinetics, and ease of shaping and manufacture, enabling appropriate pore sizes [19]. Especially, electrospun PCL membranes allow gas exchange and absorb the exudate in the wound area, thanks to its elastic morphology with interconnected porous structure. In addition, this elastic structure provides the comfort of movement in the wound area [20]. However, despite the many features mentioned above, PCL membranes negatively affect wound healing. Furthermore, PCL is highly hydrophobic like other aliphatic polyesters, which limits its use alone as a dressing material [21, 22]. Therefore, it has been shown that wound dressing materials obtained from electrospun membranes, in which synthetic or natural polymers are used as a mixture, have a synergistic effect and contribute positively to the wound healing process compared to the use of the polymers mentioned above alone [23].

Using herbs in wound dressing materials accelerates the wound healing process and reduces the necessity for demand medical drugs such as antibiotics [9, 24]. Significantly, the electrospun membranes containing plant extracts are state-of-the-art for wound dressing applications. Many plants, such as Henna, curcumin longa, moringa, honey, ginger, and propolis, have been studied with electrospun membranes for wound dressing and other biomedical applications [24–30]. *Viburnum Opulus* is also known as Gilaburu, Gileburu, Guelder-rose, Snowball Bush, European Cranberry, High Bush Cranberry, Stagbush, and Cranberry *Viburnum* [31]. *V. Opulus* is extremely important for traditional medicine treatments due to its antioxidant, antibacterial, hepatoprotective, high blood pressure-lowering, and anti-inflammatory properties [32]. In addition, it contains vitamin C, carotenoids, triterpenes, iridoids, saponins, flavonoids, and phenolic compounds such as hydroxybenzoic acids, tannins, anthocyanins, chlorogenic acid, (+)-catechin, (−)-epicatechin, cyanidin-3 glucoside, cyanidin-3-rutinoside, and quercetin [31–34]. In addition, phenolic compounds, especially quercetin, have good antibacterial properties against gram-negative and gram-positive bacteria [30].

There are several studies about the antibacterial and antioxidant effects of *V. Opulus* and its extracts in the literature. However, there is no study about *V. Opulus* containing electrospun wound dressing membranes. Our study prepared PCL/gelatin membranes containing *V. Opulus* extract using the electrospinning technique and characterized their structural and morphological properties. Antibacterial activity of *V. Opulus*-containing membranes was shown by disc diffusion technique against *E. coli* and *S. aureus* bacteria. Additionally, in vitro cell viability and cell proliferation behavior of membranes were investigated using a fibroblast cell line, and this study reported the results.

2 Materials and Methods

2.1 Materials

The polycaprolactone (PCL, average Mn = 80,000; CAS No. 24980–41-4), gelatin (derived from bovine skin, CAS No. 9000-70-8) and 1,1,1,3,3,3-hexafluoro-2-propanol (HFIP) (CAS No. 920–66-1) were purchased from Sigma-Aldrich. Methanol and agar were obtained from Merck. Inovenso NE100 (İstanbul, Turkey) model electrospinning device was used to fabricate nanofiber membranes. Cell viability was analyzed by CellTiter 96® AQueous One Solution Cell Proliferation Assay. Cell proliferation attachment was determined by DAPI (4',6-Diamidino-2-phenylindole dihydrochloride, Sigma-Aldrich). DMEM (Dulbecco's Modified Eagle Medium High Glucose) and PBS (Dulbecco's Phosphate Buffer Saline) were purchased from Biological Industries (USA). FBS (Fetal Bovine Serum), penicillin/streptomycin, and LB Broth were purchased from Gibco (USA). The fermented *V. Opulus* fruits were obtained from Kayseri, Turkey. The human fibroblast cells, *Escherichia coli*, and *Staphylococcus aureus* were donated from Erciyes University, Kayseri/Turkey (Fig. 1).

2.2 Extraction of *Viburnum Opulus*

The fermented fruits of *Viburnum Opulus* were extracted by Soxhlet extraction techniques. Initially, the fermented *V. Opulus* fruits were dried in an incubator at 40 °C. Next, 25 g of *V. Opulus* were extracted in 500 ml methanol at 100 °C for six h. Finally, the excess methanol was removed by a rotary evaporator (Buchi, Rotavapor R300). The final extract was stored at −20 °C for further experiments.

2.3 Fabrication of Electrospun Membranes

The neat PCL/gelatin membrane and PCL/gelatin membranes with *V. Opulus* extract were fabricated by electrospinning technique. Briefly, 8% (w/v) PCL/gelatin with the ratio of 9:1 (w/w) was dissolved in HFIP and stirred for 8 h. Then, different amounts of *V. Opulus* extracts (25, 35, 50%, w/v) were added to the solution. The final solutions were stirred for 12 h and were poured into a syringe. 21G needle was used for the electrospinning process, and the distance between the tip and the collector was adjusted to 15 cm. The solution flow rate was 1 m/h; the voltage was applied at 15 kV. The neat PCL/gelatin membrane was labeled as AY1,

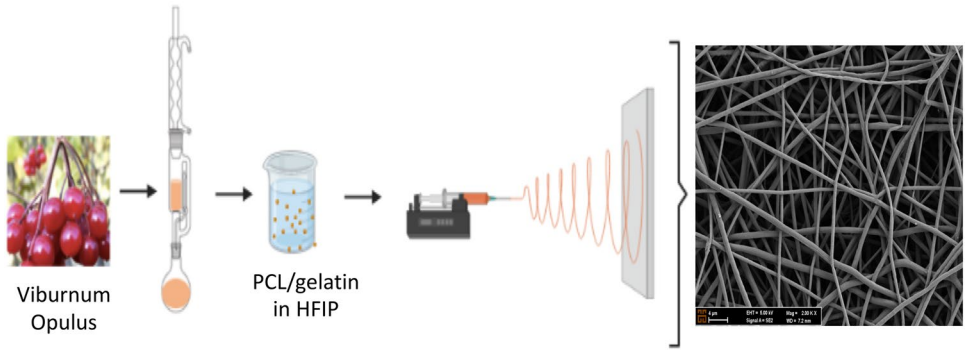

Fig. 1 Schematic representation of the membranes' fabrication

Table 1 The combination of electrospun membranes

Membrane	PCL/gelatin (%, w/v)	*Viburnum Opulus extract* (%, w/v)
AY1	8	–
AY2	8	25
AY3	8	35
AY4	8	50

and the membranes with *V. Opulus* extract were labeled AY2, AY3, and AY4, as shown in Table 1.

2.4 Characterization of Electrospun Membranes

2.4.1 Chemical Characterization

The chemical structure of the *V. Opulus* extract and electrospun membranes were characterized using Fourier Transform Infrared Spectrometer (F-TIR, Thermo Scientific Nicolet 6700) in the range of 400–4000 cm^{-1} [35].

2.4.2 Morphological Characterization

The fiber orientation and diameters were examined by Scanning Electron Microscope (SEM, Carl Zeiss EVO LS10, Germany) at magnifications 1000X, 2000X, and 3000X. The Image J software (National Institutes of Health, Bethesda, MD) was used to calculate the fiber diameters and average pore sizes of membranes from SEM images [36].

2.4.3 Contact Angle Measurement and Swelling Test

A swelling test was applied to determine the water adsorption capacity of membranes. Briefly, the membranes were immersed in distilled water for 30 min. Every 5 min, all membranes were weighed after removing the surface water with filter paper. The membranes' water adsorption percentages were calculated as shown in the below equation.

$$\mathrm{Ws}(\%) = \frac{W - Wo}{Wo} x100 \quad (1)$$

where W_o is the first weight of membranes, W is the weight of the membranes after immersion, and W_s is the water adsorption capacity percentage of membranes [35].

Water contact angle values of membranes were investigated by the sessile drop technique. It is based on the time-dependent analysis of the shape and volume of the water droplet image formed, using the Young–Laplace equation as a reference. In this analysis, the contact angle values of the membranes were determined by Contact Angle-Sessile Drop (Biolin Scientific Attention Theta Lite) measurement and compared with each other.

2.4.4 In Vitro Degradation Study

In vitro degradation study of the membranes was performed by mimicking the physiological environment of the human body. Firstly, the membranes were placed in 15 ml PBS solution and kept at 37 °C in a 100-rpm shaker incubator. After 7, 14, and 21 days, membranes were taken from PBS solution and dried to measure weight loss. The below equation calculated weight loss percentages of membranes.

$$\%\mathrm{W} = \frac{(\mathrm{Mo} - \mathrm{Mt})}{Mo} \times 100 \quad (2)$$

where M_o is the first weight of samples, M_t is the final weight of the samples after incubation, and W is the weight loss percentage of samples [36].

2.4.5 In Vitro Extract Release Study

To determine *V. Opulus* release from membranes, we followed the *V. Opulus* absorbance. Firstly, *V. Opulus* were dissolved as 0.2, 0.1, 0.05, 0.025, 0.0125 mg/ml in water and scanned between 200 and 700 nm by UV spectrophotometer. The 323 nm was chosen as a specific nm value for *V. Opulus*. Secondly, *V. Opulus*-containing membranes were placed into a 15 ml PBS solution. Then, on 1, 2, 3, 4, 5, 6,

12, 24, 48, and 72 h 1 ml sample was withdrawn from the PBS solution, and 1 ml fresh PBS was added to the medium. The absorbance of the withdrawn samples was measured at 323 nm. The cumulative release of *V. Opulus* was calculated using the following equation.

$$\text{Cumulative release}\,(\%) = 100 \times \frac{(Vm \times C(n)) + (1ml \times \sum C(n-1))}{Mo} \quad (3)$$

where Vm is the volume of release medium, C(n) is the extract amount at time n, C(n-1) is the cumulative extract amount at a time (n-1), and Wo (mg) is the amount of loaded extract on the membrane [35–37].

2.4.6 In Vitro Antibacterial Activity Test

The antibacterial activity of membranes was evaluated by the Kirby–Bauer disk diffusion test against *E. coli* and *S. aureus* bacteria. Firstly, the bacteria solution was streaked using a sterile swab on the LB agar plate. Next, membranes and ampicillin antibiotic discs were located on the agar plate. After incubation for 16 h at 37 ° C, zone diameter was measured to show the antibacterial activity of the membranes [37].

2.4.7 Mechanical Characterization

The uniaxial tensile tests were applied to analyze the mechanical properties of membranes. Firstly, each membrane was cut with 20 mm width, 60 mm length, and 0.02 mm thickness. Tensile strengths and elongation at the break of membranes were determined by tensile test using an Autograph AGS-X 10 kN (Shimadzu, Japan) device. The strain rates of 1×10^{-2} s^{-1} were applied to the tensile tests at room temperature [38]. The stress–strain curve, tensile strength, elongation at the break, and Young's modulus were calculated from Force–Stroke results given by the TRAPEZIUM X program.

2.4.8 In Vitro Cell Viability, Attachment, and Proliferation Study

The electrospun membranes' cell viability (%), attachment, and proliferation assessments were investigated using a human dermal fibroblast cell line (ATCC PCS-201–012™) with in vitro assays. The cell viability of the human fibroblast cells on the electrospun membranes with and without *V. Opulus* were investigated by MTS assay (Cell Titer 96® AQueous One solution; G3581, Promega, USA). This MTS assay is a colorimetric assay which is determine the number of viable cells in proliferation or cytotoxicity assays. The MTS reagent contains a tetrazolium compound [3-(4,5-dimethylthiazol-2-yl)-5-(3-carboxymethoxyphenyl)-2-(4-sulfophenyl)-2H-tetrazolium]. The working principle of the MTS assay is that yellow tetrazolium transforms into purple formazan crystals only in living cells and absorbance records at 490 nm in 96-well plate. First, the fibroblast cells were cultured in cell culture plates with DMEM-High Glucose medium supplemented with 10% FBS and 1% penicillin/streptomycin in an incubator at 37 °C with 5% CO_2. The membranes were cut and sterilized with 70% ethanol overnight and UV light for 1 h. After sterilization, membranes were kept in DMEM-High Glucose media for 15 min. Then, the membranes were placed into 96 well plates, and 10^4 cells were seeded on the membranes. After the incubation for 24 h, 48 h, and 72 h, membranes were removed from each plate. 20 µl MTS reagent was added to each plate and incubated for 2.5 h. Then, absorbance was measured at 490 nm using a microplate reader (Varioskan, Thermo Scientific) [36].

For the fibroblast cell attachment and proliferation assessments, membranes were placed into 96 well plates, and 10^4 cells/well were seeded onto the membranes and incubated for 24 h, 48 h, and 72 h. Following days, the membranes were removed from the plate and rinsed with PBS to remove the non-attached cells. Then the cells on the membranes were fixed with glutaraldehyde solution (2.5%, v/v) and washed in PBS solution. To determine the cell nuclei on membranes DAPI staining was used (DAPI Dye, Thermo Fisher Scientific, D1306). The 20 µl DAPI dye solution (300 Nm) was added to each membrane surface and incubated for 5 min with protection from the light. After washing with PBS, membranes were investigated under the fluorescence microscope [37].

2.4.9 BET Surface Area Analysis

The Brunauer–Emmett–Teller (BET) surface area of membranes were investigated with a surface area analyzer (Micromeritics, Gemini VII Surface Area and Porosity). The physical adsorptions and desorption of nitrogen gas were calculated at 77 K. The membranes were degassed in a vacuum at room temperature for 24 h before the BET analysis. The BET surface area and pore volume of membranes were determined by the BET analyzer.

2.4.10 Thermal Analysis

To determine the thermal properties of membranes, the thermal analysis (TGA, Perkin Elmer, USA) analysis was applied between 30 and 400 °C at a heating rate increased to 10^0C in a minute.

3 Results and Discussions

3.1 Chemical Characterization

Figure 2 indicates the FT-IR spectra of membranes *and V. Opulus* fruit extract. The broad absorption peak nearly at 3315 cm^{-1} corresponds to the stretching vibration of the OH in H-bonded alcoholic and phenolic compounds [39]. Additionally, the C-O stretching vibration of the phenolic compounds was observed at 1236 cm^{-1}. The peaks at 2917, 1717, and 1600 cm^{-1} correspond to the vibration of C-H stretching, carbonyl group vibration, and C = C stretching vibration, respectively [40, 41]. According to the literature, the FT-IR result showed all characteristics peak of *V. Opulus.* On the other hand, PCL characteristic peaks appeared at 2942 cm^{-1} and 2863 cm^{-1} from asymmetric and symmetric CH_2 stretching, respectively. PCL also includes carbonyl stretching at 1727 cm^{-1}, C–O and C–C stretching at 1293 cm^{-1}, and asymmetric COC stretching at 1240 cm^{-1} [42]. Gelatin includes amide I-II proteins which attribute C = O stretching at 1650 cm^{-1} and coupling of bending of N–H bond and stretching of C–N bonds at 1540 cm^{-1}. Additionally, a random coil and a-helix conformation of gelatin attribute the amide I band at 1650 cm^{-1} [43]. The increase of *V. Opulus* concentration in membranes shows a more significant change in the broad absorption peaks.

3.2 Morphological Characterization

The morphology of electrospun membranes was investigated using SEM, where the representative images are given in Fig. 3. Since the electrospinning solution was a homogeneous extract-polymer mixture, the extract was embedded into the fibers. This is demonstrated by FTIR analysis and SEM images in Figs. 2 and 3. According to the SEM images, PCL/gelatin electrospun membranes have uniform fiber distribution with no bead formation [42]. The average fiber diameters and pore sizes were calculated from SEM images using ImageJ software and indicated as a bar chart in Fig. 4a and b. There is a continuous rise in the diameter of nanofibers by increasing the concentration of *V. Opulus.* As shown in Fig. 4a, the fiber diameter of AY1 was calculated as 591 nm, while the average fiber diameters of AY2, AY3, and AY4 containing 25, 35, and 50% (w/v) *V. Opulus,* were calculated as 647 nm, 1014 nm and 1222 nm, respectively. The rising average fiber diameter may be due to the increased viscosity of the polymer solution [43–45]. The electrospinning process is sensitive to solution viscosity. The increase in solution viscosity resulted in a larger fiber diameter [43, 44]. According to the literature, the electrospun PCL/gelatin fibers' diameters range from approximately 300 to 600 nm. Chong et al.'s study showed that the average fiber diameter of PCL/gelatin electrospun membrane is 470 ± 120 nm [46]. Another study mentioned that 440 ± 170 nm fiber diameter was measured from 6% (w/v) PCL/gelatin electrospun membrane [47]. Zhang et al.'s study showed that the addition of *Quercetin* extracts increased fiber diameters of PCL/gelatin membrane from 312.02 nm to 365.33 nm [48]. Amna et al. mentioned that the fiber diameter of PCL membranes increased from 300 ± 50 nm to 500 ± 20 nm by loading C*amptothecin*. They highlighted that the enlargement of fibers is an evidence for C*amptothecin* integration inside the PCL nanofibers [49]. Khan et al.'s study showed

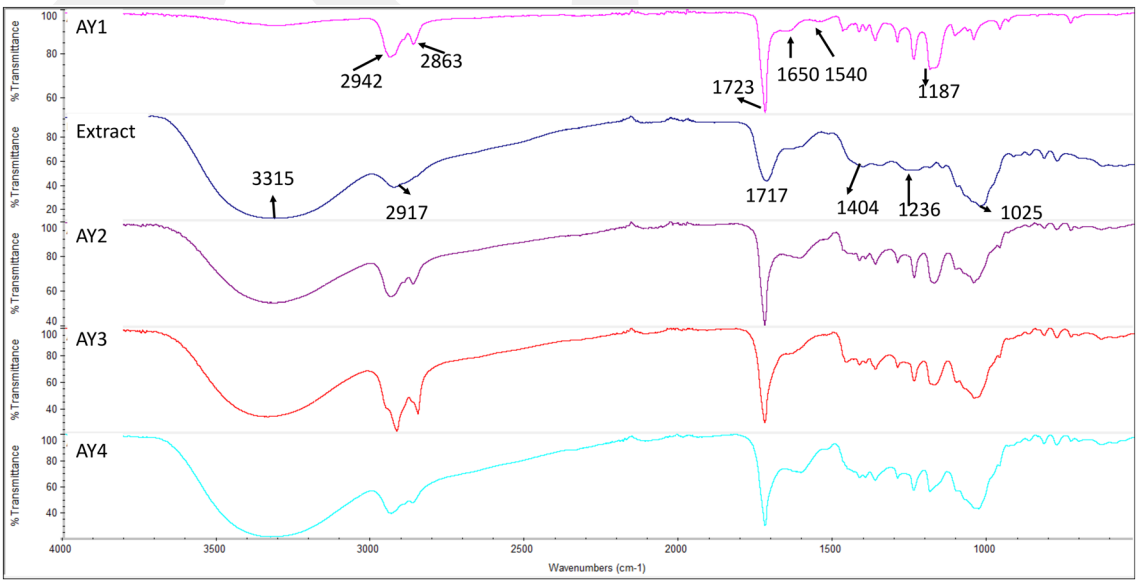

Fig. 2 FT-IR spectra of *V. Opulus* extract and the electrospun membranes

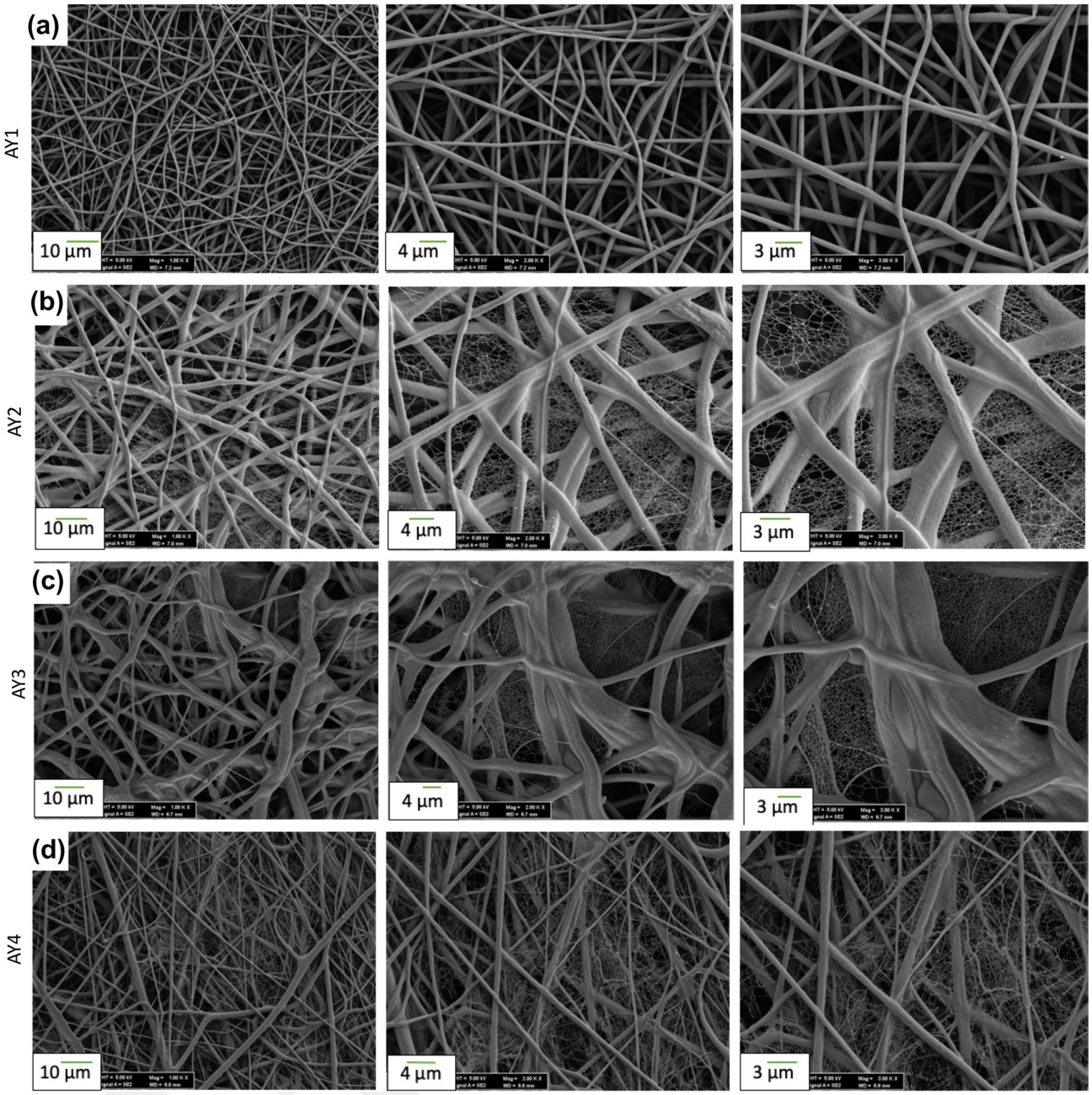

Fig. 3 SEM images of **a** AY1, **b** AY2, **c** AY3, and **d** AY4, magnification of 1000X, 2000X and 3000X, respectively

that the addition of *Phoenix dactylifera L.* extracts increased fiber diameters [50]. In another study, *Tecomella Undulata* extract increased fiber diameters of PCL/PVP membranes as 0.35 µm to 0.65 µm [51]. The average pore sizes of membranes are 10.128 ± 6.7 µm, 8.303 ± 3.4 µm, 7.262 ± 3.1 µm, and 8.362 ± 2.8 µm for AY1, AY2, AY3, and AY4 as seen Fig. 4b, respectively. The *V. Opulus* narrowed the pores in membranes due to the presence of extract between fibers as seen in SEM images in Fig. 3. Also, the increasing fiber diameters decrease the pore sizes [49, 50]. According to Balaji et al. 4–50 µm pore size is effective for the infiltration of nutrients and gas exchange in wound area [52]. According to the literature, it was concluded that the morphology, average fiber diameters and pore sizes of PCL/gelatin membranes given herein are consistent with the literature.

3.3 Contact Angle Measurement and Swelling Test

Figure 4c and 4d represent the membranes' contact angle measurements and swelling test results. Contact angle values

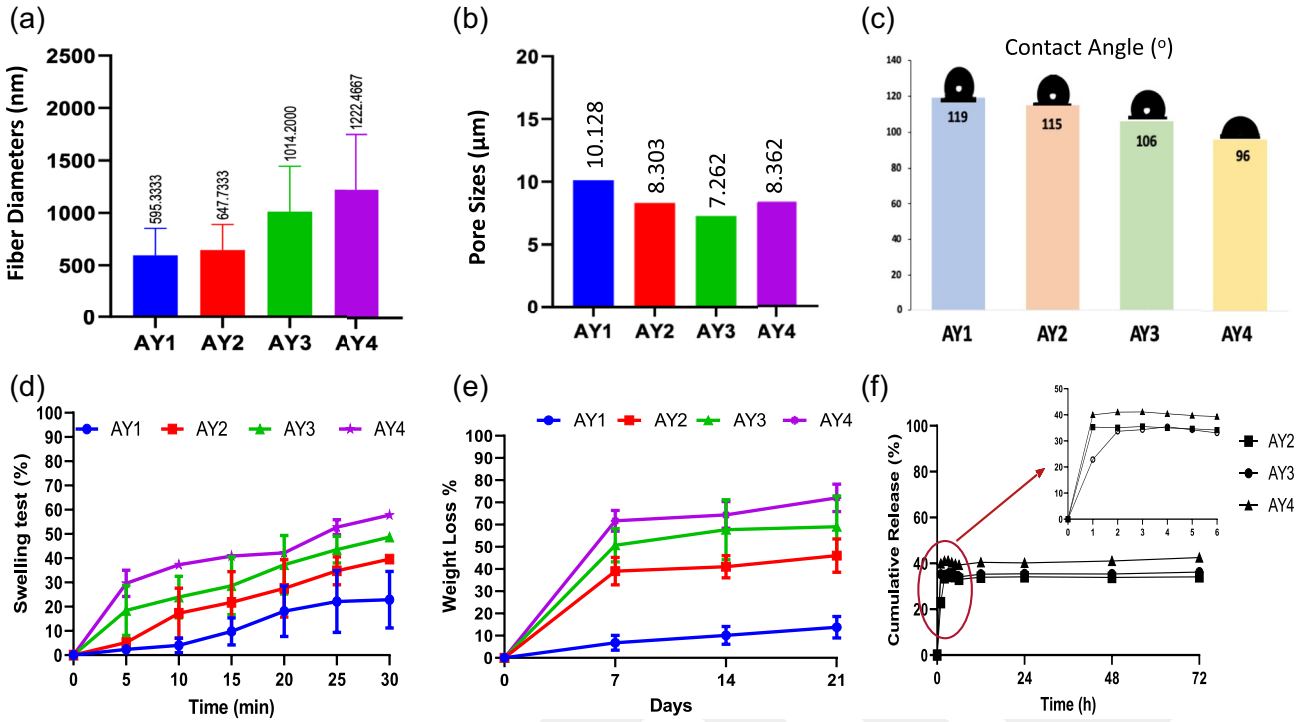

Fig. 4 **a** The average fiber diameters, **b** average pore sizes, **c** contact angle, **d** swelling test, **e** weight loss study, and **f** cumulative release studies of membranes

were measured as 119°, 115°, 106°, and 95° for AY1, AY2, AY3, and AY4, respectively. The increasing *V. Opulus* concentration improved the hydrophilicity of membranes thanks to the phenolic compounds in its structure. The phenolic compounds include hydrophilic side chains such as galloyl, hydroxyl, glucoside, and gallate [34]. Similar behavior shown in Khan et al.'s study, the hydrophilicity of electrospun membranes improved by the addition of the *Ajwa-Dates* extract as 143° to 84° [50].

Membranes showed the 22,84%, 39,63%, 48,71% and 57,75% swelling behaviors, AY1, AY2, AY3, and AY4, respectively. The increasing *V. Opulus* concentration significantly increased the water adsorption capacity compared to the neat membrane. The high porosity of the electrospun nanofibers resulted in a high swelling capacity [42, 46]. Similar swelling behavior was observed on the PLGA/gelatin membrane containing *Hypericum* plant extract. The swelling ratio increased by adding *Hypericum* plant extract [37]. Swelling capacity and hydrophilicity are important criteria for wound dressing materials [53]. According to the swelling test, all membranes showed suitable water adsorption capacity.

3.4 In Vitro Degradation Study

Figure 4e represents the in vitro degradation results of membranes. Membranes lost their weights by 13,7%, 46%, 59%, and 72% within 21 days, respectively, AY1, AY2, AY3, and AY4. The weight loss of membranes corresponding to PCL/gelatin hydrolytic degradation due to hydrolytic cleavage of ester groups on PCL [19]. Also, gelatin degrades under physiological conditions because it contains degradable sites [54]. *V. Opulus* extract containing membrane's degradations ratio is higher than AY1. The high-water uptake capacity can be explained by resulting in more cleaved bonds. After the first week, membranes exhibited a stable weight loss due to their completed water uptake and dissolved extract into the water. The phenomenon knowns as 'burst release' causes a high amount of drug release the first time due to the burst effect [55]. *V. Opulus* extract containing membranes could be more susceptible to burst effect due to high water uptake capacity, which correlated swelling result in Fig. 4d. Hadisi et al. observed that adding the henna extract to a membrane increased the degradation rate of electrospun membranes [56]. Degradation rates of membranes attribute to the *V. Opulus* containing membranes, which are suitable for wound dressing materials.

3.5 In Vitro Extract Release Study

Figure 4f indicates that *V. Opulus* extract released approximately 22%, 35%, and 39% from AY2, AY3, and AY4 in the first hour, respectively. The release curve can be divided into two parts, a burst release phase and a stagnant release

phase [57]. Within the first hour, the burst effect caused the burst release of extract from membranes. After the first hour, the extract is released steadily in the stagnant release phase. There are no significant differences between AY2, AY3, and AY4. A similar result was shown in Canga et al.'s study. The rapid initial release of the *V. Opulus* was shown from the electrospun Cellulose Acetate/Gum Arabic membrane. Approximately 30% of the *V. Opulus* extract was released in the first 1 h, 60% was released in the first 10 h, then stabilized after 10 h [45]. Aksit et al. observed that the *Hypericum* extract was released 80% from electrospun PLGA/gelatin membranes in the first 24 h. The absorption of extract content on this membrane surface causes a rapid dissolution in the PBS [37]. In another study, *Curcumin* was shown to have a % 40 initial burst release in the first hours and followed slow release up to %85 within 10 days [58]. Furthermore, a %80 burst release of *Garcinia Mangostana* extract was seen in the first hour due to swelling of the electrospun membrane in water [59]. In the literature, Camptothecin drug released as 55% within 70 h from the PCL membrane [49]. In Suganya et al.'s study, *Tecomella Undulata* extract was released as 40% within 24 h from the PCL/PVP membrane [51]. In Cortez et al.'s study, the embelin released 80% within 8 h from PCL membranes [60]. According to Khan et al. the release behavior depends on some parameters such as the fiber diameters, hydrophilicity of membranes, and the drug or extract distribution inside fibers. The drug migrates towards the fiber surface and may cause the rapid-release profile [50]. The release behavior of *V. Opulus* from membranes can be explained by these hypotheses. As a result, the cumulative release behavior of *V. Opulus* from electrospun PCL/gelatin membrane was correlated with the literature.

3.6 In Vitro Antibacterial Activity

The antibacterial activity test results against gram-positive and gram-negative bacteria were summarized in Fig. 5. According to the results, no bacterial activity was observed for AY1 against both bacteria types. After adding *V. Opulus* to membranes, the inhibition zone for *E. coli* rose to 25 mm in AY2, 30 mm in AY3, and 36 mm in AY4. Similar behavior was observed for *S. Aureus*. The inhibition zones' sizes increased with the content of *V. Opulus*, starting at 14 mm in AY2, 18 mm in AY3, and 25 mm in AY4. Our results showed that adding *V. Opulus* to the membranes provides antibacterial properties against *E. coli* and *S. aureus*. Laima et al. demonstrated that the fruit juice of *V. Opulus* showed 22 mm and 24 mm zone inhibition against *E. coli* and *S. aureus* bacteria, and the ethanol extract of *V. Opulus* showed 18.8 mm and 18.6 mm zone inhibition against *E. coli* and *S. aureus* bacteria [61]. Also, the methanol extract of *V. Opulus* has been proven to have an antibacterial effect against gram-negative and positive bacteria in literature [30, 62]. As mentioned in the introduction section, *V. Opulus* contains abundant bioactive compounds such as vitamin C, carotenoids, triterpenes, iridoids, saponins, flavonoids, and phenolic compounds which are hydroxybenzoic acids,

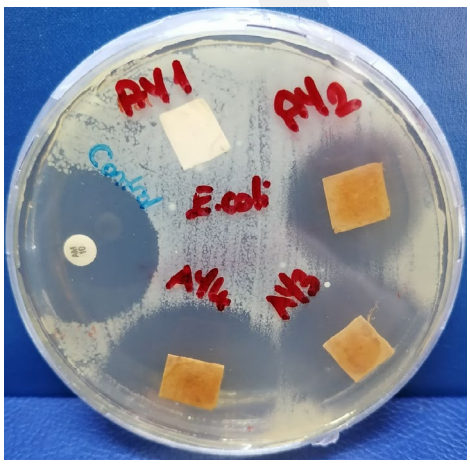

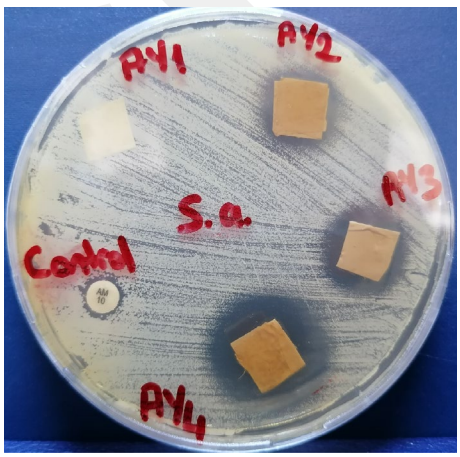

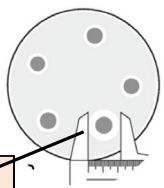

Bacteria	Control	AY1	AY2	AY3	AY4
Escherichia coli	32 mm	0	25 mm	30 mm	36 mm
Staphylococcus aureus	8 mm	0	14 mm	18 mm	25 mm

Fig. 5 Antibacterial activity of AY1, AY2, AY3, and AY4

tannins, anthocyanins, chlorogenic acid, (+)-catechin, (−)-epicatechin, cyanidin-3 glucoside, cyanidin-3-rutinoside, and quercetin [31–34]. The presence of these bioactive compounds provides the antibacterial and antioxidant property as known in the literature [32]. The presence of bioactive phenolic compounds such as chlorogenic acid and procyanidins, provide antibacterial effect by effecting on bacterial cell wall membrane [32]. Also, the polyphenols include hydroxyl groups which have a high binding affinity with bacterial cell membrane proteins. Therefore, phenolic compounds provide antibacterial activity by interacting with bacterial cell wall membranes and changing the membrane rigidity, permeability, and integrity [63]. In this study, the antibacterial activity of membranes containing *V. Opulus* was proven against *E. coli* and *S. aureus* due to its components, such as phenols, flavonoids, chlorogenic acid, and procyanidins [32–34, 64–66].

3.7 Mechanical Characterization

Figure 6 indicates the engineering stress–strain curves, Young's modulus, ultimate tensile strength, and strain at breaks of membranes. There was a linear increase of Young's modulus value of membranes AY1 to AY4. Electrospun PCL/gelatin membrane without *V. Opulus* showed 43,352 MPa Young's modulus value. The addition of *V. Opulus* extract increased Young's modulus value to 44.94 MPa, 46.509 MPa, and 59.6 MPa. The addition of *V. Opulus* extract to PCL/gelatin membrane increased the average fiber diameters and can result in increasing mechanical properties. Adding 25% and 35% of *V. Opulus* extract to PCL/gelatin membranes decreased its ultimate tensile strength to 0,782 MPa and 0,821 MPa. However, the 50% amount of *V. Opulus* extract containing membrane increased its tensile strength to 1,8676 MPa. Elongation (%) of AY1 was about 124.9%, and it was the maximum ductility compared to AY2, AY3, and AY4. Like ultimate tensile strength, the ductility percentage decreased when adding *V. Opulus* extract. The possible reason can be due to the nature of *V. Opulus* extract. Several factors, such as composition, fiber diameter, structure, and interaction between nanofibers, are of great importance in determining the mechanical properties of electrospun membranes [67]. The obtained results agreed with Hadizadeh et al., when they added 3% and 5% *Curcumin* extract to PCL/gelatin, they found the tensile strength value to be 0.83 and 0.6 MPa, which are very close to our values of AY2 and AY3 [68]. A study observed a similar behavior; adding *Calendula officinalis* extract and *Gum Arabic* decreased the flexibility and elongation of PCL nanofibers [69]. Also, Rad et al. mentioned that the suitable tensile strength range for nanofibrous membranes is 0.8 -18.0 MPa for skin applications [70]. In another study, adding *Biophytum sensitive* extract into PCL nanofibers reduced the elongation at break (%) by 2.3 times [71]. When we compared membranes used for wound healing material in the literature, the whole samples' mechanical property values were suitable for wound dressing material [72].

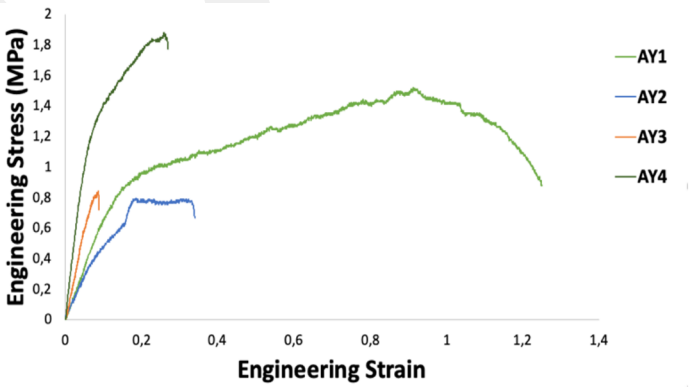

Fig. 6 Stress–Strain Curves and data summary of the tensile test analysis of AY1, AY2, AY3, and AY4

Membranes	Young's Modulus (MPa)	Ultimate Tensile Strength (MPa)	Strain/Elongation at Break (%)
AY1	43,352	1,501	124,9
AY2	44,94	0,782	33,58
AY3	46,509	0,821	8,75
AY4	59,6	1,8676	26,75

3.8 In Vitro Cell Viability, Attachment and Proliferation Studies

Cell viability of human dermal fibroblast cells on membranes was investigated by MTS assay at 24, 48, and 72 h are given in Fig. 7. The figure shows that the cell viability was over 95% for all membranes at 24, 48, and 72 h. Also, the cell viability ratios of *V. Opulus*-containing membranes are higher than AY1 and control plates. In 24 h incubation, AY4 had high viability of 132%, while AY1 had a viability of 95%. The hydroxyl groups of *V. Opulus* neutralize the free radicals in the cell environment by transferring the hydrogen atoms to free radicals. The neutralizing of free radicals decreases the oxidative stress around the cells [73]. The antioxidant activity of *V. Opulus* was proved in literature against hydroxyl, peroxyl, and superoxide free radicals [33, 34, 74]. The improving cell viability on membranes containing *V. Opulus* can be explained by the antioxidant effect of *V. Opulus* [34]. Altun et al. demonstrated the antioxidant effect of *V. Opulus* by scavenging free radicals [75]. Zakłos-Szyda et al. supported that using 10% and 25% of *V. Opulus* extract increased the cell viability up to 100% [34]. In Jafari et al.'s study, electrospun PCL/gelatin/ZnO_2 membranes represented higher cell viability than their control plate. It can be explained by the physical and biological properties of the membrane, such as high porosity, microstructural similarity to native ECM, and bioactivity [44]. Finally, these results showed that adding *V. Opulus* extract to electrospun membranes had no toxic effect on fibroblast cells. Therefore, the PCL/gelatin electrospun membranes containing *V. Opulus* have great potential to wound dressing applications.

The human dermal fibroblast cells adhesion and proliferation on the membranes at 24, 48, and 72 h was investigated by DAPI staining in Fig. 8. DAPI staining is an easily applicable technique to visualize cell nuclei under fluorescence microscopy. Basically, 4′,6-diamidino-2-phenylindole (DAPI) is a fluorescence dye and can pass from the cell membrane and strongly bind to Adenozine-Thimine regions of DNA via electrostatic interactions. The DAPI-stained cells can be investigated under fluorescence microscopy in terms of the adhesion and proliferation behavior of cells [76]. As clearly observed from the images, adding *V. Opulus* to the membrane significantly increased cell proliferation and adhesion on the membranes. While the spread and adhesion of fibroblast cells to the membranes were weak at 24 h, their adhesion and spread increased at 48th and 72nd hours. Additionally, increasing the concentration of *V. Opulus* increased cell adhesion. The increases in cell adhesion can be explained by due to the presence of functional groups into *V. Opulus* and more hydrophilicity than neat membrane [77]. Hadisi et al. mentioned that the *Henna* extract-containing membranes increased fibroblast proliferation due to containing flavonoids which promotes fibroblast proliferation [52]. Also, Bashur et al. reported that an increased diameter and degree of orientation of electrospun fibers contributed to the enhanced adhesion and aspect ratio of fibroblasts [78]. The increased hydrophilicity of membranes by *Ajwa-Dates* extract, improved the cell proliferation of PCL membranes in the literature [50]. Kim et al. Mentioned that the increasing hydrophilicity improves the cell adhesion on membranes [79]. Therefore, the membranes both effect of containing *V. Opulus* and hydrophilicity created a synergistic effect, and increased cell adhesion and viability.

3.9 BET Surface Area

The BET surface area and porosity analysis of membranes were presented in Table 2. The AY1 has 3.3071 ± 0.1481 (m^2/g) BET surface area while AY2, AY3, and AY4 has 1.1557 ± 0.0525, 0.3728 ± 0.0393 and 0.9221 ± 0.0400, respectively. The pore volumes of membranes are 0.001874 cm^3/g, 0.001694 cm^3/g, 0.001166 cm^3/g and 0.001500 cm^3/g for AY1, AY2, AY3, and AY4, respectively. The *V. Opulus* decreased the BET surface area and pore volumes of PCL/gelatin electrospun membranes. It can be explained by the extract embedded between fibers and resulted decrease in BET surface area and pore volumes. Also, the fiber diameters of extract-containing membranes are higher than neat

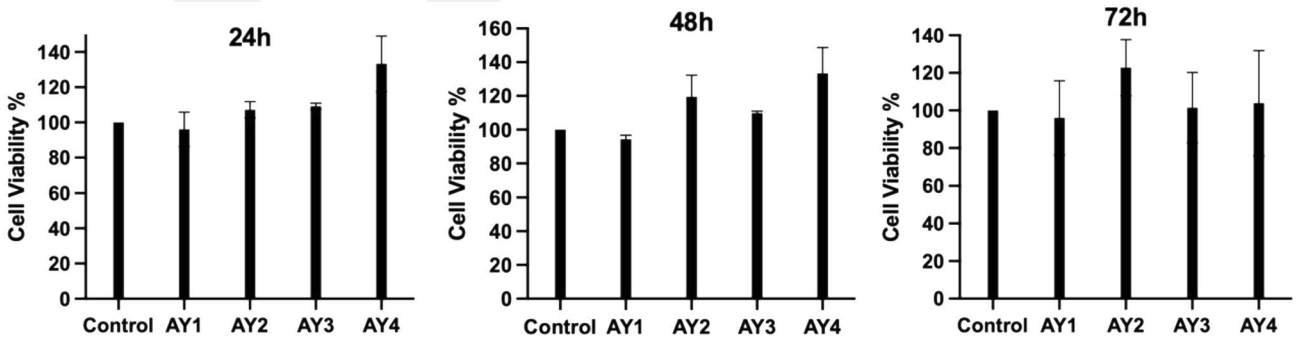

Fig. 7 Cell Viability of AY1, AY2, AY3, and AY4 at 24 h, 48 h, and 72 h

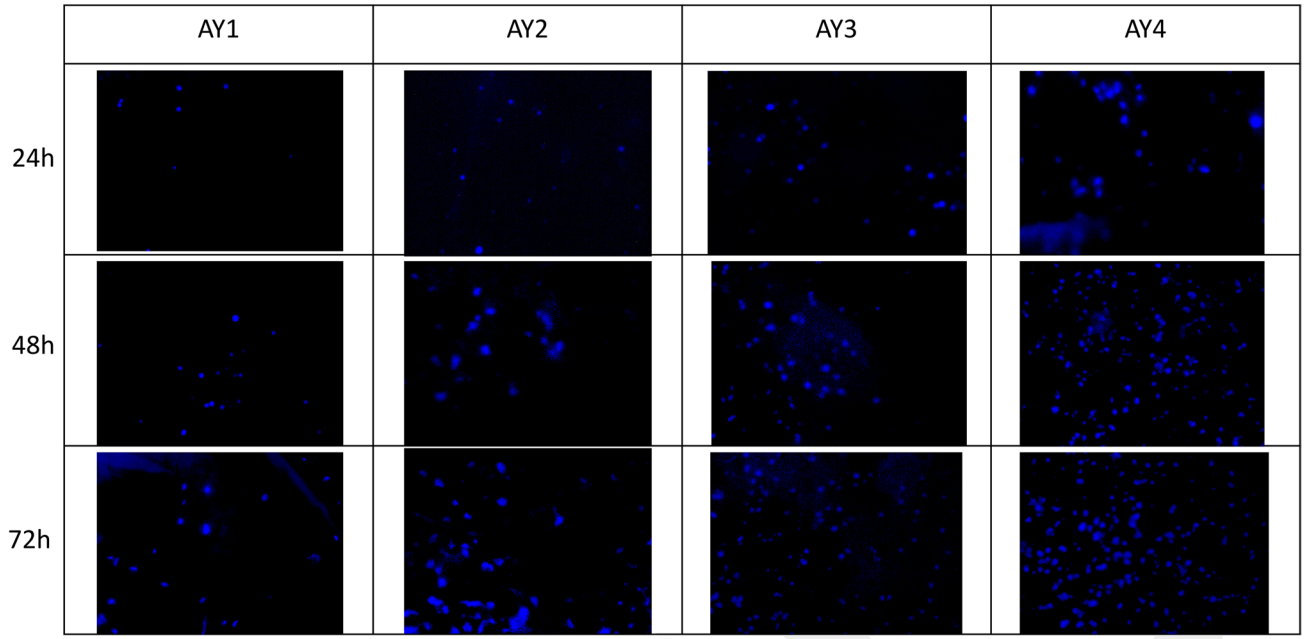

Fig. 8 DAPI staining of AY1, AY2, AY3, and AY4 at 24 h, 48 h, and 72 h

Table 2 BET surface area of membranes

Membranes	BET Surface Area (m^2 /g)	Pore Volume by BET (cm^3/g)
AY1	3.3071 ± 0.1481	0.001874
AY2	1.1557 ± 0.0525	0.001694
AY3	0.3728 ± 0.0393	0.001166
AY4	0.9221 ± 0.0400	0.001500

membrane. The increasing fiber diameter decreases the BET surface area and pore volumes of electrospun membranes [80]. In the literature, PCL/gelatin has approximately 3.274 m^2/g BET surface area and 0.011 cm^3/g pore volume [81]. AY1 showed a very similar BET surface area with the literature's PCL/gelatin membranes. In the Can-Herrera' study, the fiber diameters of PCL membranes increased from 775 nm to 1376 nm approximately, resulted in a decrease in BET surface area from 6 m^2/g to 3.8 m^2/g. They demonstrated the increasing fiber diameters corresponding to decreasing in the BET surface area [82]. In Wei et al.'s study, when the drug particle size increased, the BET surface area decreased due to the particle occupied the pore space [83].

3.9.1 Thermal Analysis

The thermal properties of PCL/gelatin electrospun membranes with and without *V. Opulus* were investigated by using TGA as seen in Fig. 9. TGA thermograms showed that AY1 started to degrade at about 338.72 °C, associated with the PCL/gelatin degradation. The *V. Opulus*-containing membranes were shown two degradation peaks which are approximately at 170 °C and 360 °C in TGA thermograms. At the end of 450 °C AY1 degraded approximately %86. AY2, AY3 and AY4 showed similar degradation behavior as 30–35% at 150–200 °C, and 40–45% at 250–450 °C. It may be explained by secondary metabolites especially phenolic compounds into *V. Opulus* extract [84]. In addition, a similar degradation behavior was seen in Suganya et a.'s study. The *Tecomella Undulata* extract containing PCL/PVP membrane showed two degradation peaks between 212–281 °C and 385–413 °C in TGA thermograms. They explained that the interaction between the *Tecomella Undulata* extract and polymer changed the PCL/PVP membrane's thermal stability [51]. In another study, Doostmohammadi et al. showed that PCL/gelatin started to degrade at nearly 300 °C according to its TGA thermogram [85]. When compared with the literature, plant extract generally shows similar behavior associated with the thermal decomposition of extract compounds such as carbohydrates and organic compounds [86]. Fernandes et al. mentioned that the reproducible peaks of plant extracts in thermal analysis are very difficult due to the interaction of extract presence substances. The degradation products of extract may be formed with different concentrations by the heating process [84]. In addition, the impurity of the extract is another difficulty for thermal analysis of the extract due to its directly affected the enthalpy [86]. Barbosa et al. mentioned that the *Aloe Vera* extract crosslinked membranes started the thermal degradation at 150°C due to formed decomposition from breaking of molecular structure

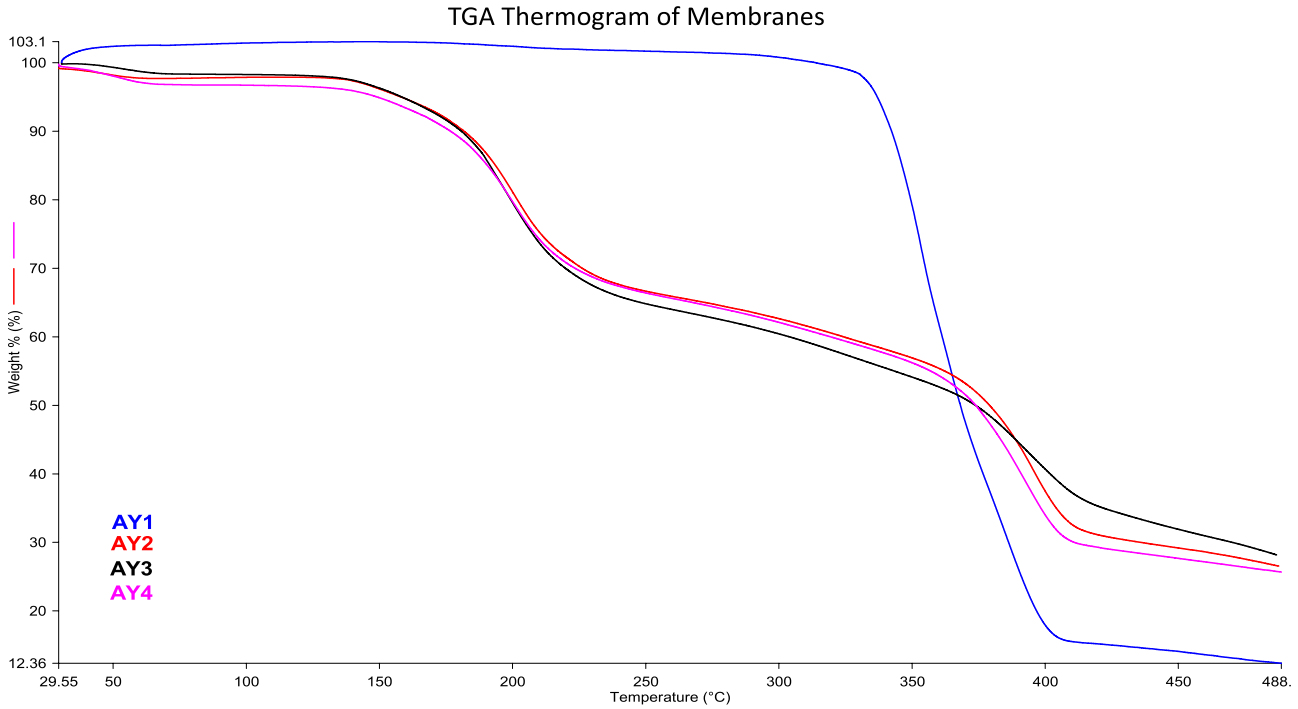

Fig. 9 TGA thermogram of membranes

and disintegration between the intermolecular bonds [87]. As a result, *V. Opulus*-containing membranes are stable enough to withstand heat exposure during decontamination processes in medical applications.

4 Conclusion

This study investigated the PCL/gelatin electrospun membranes containing *V. Opulus* extract possessing different amounts (25, 35, 50%, w/v) as an antibacterial wound dressing. We fabricated novel *V. Opulus* containing electrospun membranes with bead-free and uniform fiber structure, appropriate porosity, and mechanical strength. The average fiber diameters of neat and extract-containing membranes were measured as 591 nm (neat), 647 nm (25%, w/v), 1014 nm (35%, w/v), and 1222 nm (50%, w/v) showing that an increase in *V. Opulus* amounts increased fiber diameters of the membranes. Adding *V. Opulus* extract into the PCL/gelatin membranes increased the water adsorption capacity from 22.84% to 57.75%, and reduced the contact angle values from 119° to 95°. The degradation ratio of *V. Opulus*-containing membranes was higher than the neat membrane due to the release of *V. Opulus* from the membrane caused a reduction of membranes' weight, 72%, 59%, 46%, and 13,7%, respectively. According to the release study results, approximately 40% of *V. Opulus* was released from membranes in the first 24h. Membranes containing *V. Opulus* showed excellent antibacterial activity with the formation of inhibition zones of 25 mm to 36 mm against *E. coli* and 14 mm to 25 mm against *S. aureus*. The biocompatibility of membranes was evaluated by MTS assay, and *V. Opulus* extract did not show any toxic effect on fibroblast cells. The fibroblast proliferation and adhesion of extract-containing membranes are higher than the neat membrane. Our results significantly approve that *V. Opulus* containing electrospun PCL/gelatin membranes can be a promising material for wound dressing applications.

Acknowledgements The authors would like to thank the Turkey Council of Higher Education because Adile Yuruk is a scholarship of YÖK 100/2000. Also, the authors would like to thank the TUBİTAK BİDEB 2211-A program for Adile's scholarship. Finally, the authors would like to thank Dr. Pınar Sağıroğlu for the bacteria donation from Erciyes University.

Declarations

Conflict of interest The authors reported no potential conflict of interest.

References

1. D. Simoes, S.P. Miguel, M.P. Ribeiro, P. Coutinho, A.G. Mendonca, I.J. Correia, Eur. J. Pharma Bio **127**, 130 (2018)

2. S. Chen, B. Liu, M.A. Carlson, A.F. Gombart, D.A. Reilly, J. Xie, Nanomedicine **12**, 1335 (2017)
3. A.J. Rosenbaum, S. Banerjee, K.M. Rezak, R.L. Uhl, J. Am. Acad. Orthop. Surg. **26**, 833 (2018)
4. C.K. Sen, Adv. Wound Care **8**, 39 (2019)
5. E.A. Gantwerker, D.B. Hom, Facial Plast. Surg. Clin. North. Am. **19**, 441 (2011)
6. G. Han, R. Ceilley, Adv. Ther. **34**, 599 (2017)
7. P.H. Wang, B.S. Huang, H.C. Horng, C.C. Yeh, Y.J. Chen, J. Chin. Med. Assoc. **81**, 94 (2018)
8. G.M. Lanno, C. Ramos, L. Preem, M. Putrins, I. Laidmae, T. Tenson, K. Kogermann, ACS Omega **5**, 30011 (2020)
9. P. Fatehi, M. Abbasi, J. Tissue Eng. Regen. Med. **14**, 1527 (2020)
10. J. Cameron, Nurs. stand. *(R. Coll. Nurs. (G. B.): 1987),* 19, (2004).
11. L.G. Ovington, J. Home Care Hosp. Prof. **20**, 368 (2002)
12. F. Pourhojat, M. Sohrabi, S. Shariati, H. Mahdavi, L. Asadpour, Res. Chem. Intermed. **43**, 297 (2017)
13. D. Li, Y. Xia, Adv. Mater. **16**, 1151 (2004)
14. S.P. Miguel, D.R. Figueira, D. Simões, M.P. Ribeiro, P. Coutinho, P. Ferreira, I.J. Correia, Coll. Sur. B: Biointerfaces **169**, 60 (2018)
15. M. Szycher, J.A. Setterstrom, J.W. Vincent, G. Battistone, J. Biomater. Apl. **1**, 274 (1986)
16. W.J. Li, R. Tuli, C. Okafor, A. Derfoul, K.G. Danielson, D.J. Hall, R.S. Tuan, Biomaterials **26**, 599 (2005)
17. T. Velnar, L. Gradisnik, Med. Arch. **72**, 444 (2018)
18. M.S. Khil, D. Cha, H.Y. Kim, I.S. Kim, N. Bhattarai, J. Biomed. Mater. Res. Part B Appl. Biomater. **67**, 675 (2003)
19. M.A. Woodruff, D.W. Hutmacher, Prog. Polym. Sci. **35**, 1217 (2010)
20. N.T. Thanh, M.H. Hieu, N.T.M. Phuong, T.D.B. Thuan, H.N.T. Thu, V.P. Thai, T.D. Minh, H.N. Dai, V.T. Vo, H.N. Thi, Mater. Sci. Eng. C **91**, 318 (2018)
21. I. A. Isoglu, *Bitlis Eren Uni. Fen Bilimleri Dergisi,* 8, 1029, (2019).
22. M. Mir, M.N. Ali, A. Barakullah, A. Gulzar, M. Arshad, S. Fatima, M. Asad, Prog. Biomater. **7**, 1 (2018)
23. M. Abedalwafa, F. Wang, L. Wang, C. Li, Rev. Adv. Mater. Sci. **34**, 123 (2013)
24. I. Yousefi, M. Pakravan, H. Rahimi, A. Bahador, Z. Farshadzadeh, I. Hariri, Mater. Sci. Eng. C. **75**, 433 (2017)
25. A. Oryan, E. Alemzadeh, A. Moshiri, Biomed. Pharmacother. **98**, 469 (2017)
26. A. Oryan, E. Alemzadeh, A. Moshiri, J. Tissue Viability **25**, 98 (2016)
27. A. Oryan, E. Alemzadeh, A. Moshiri, J. Wound Care **26**, 5 (2017)
28. S.K. Saikaly, A. Hachemoune, Am. J. Clin. Dermatol. **18**, 237 (2017)
29. C.Y. Chin, J. Jalil, P.Y. Ng, S.F. Ng, J. Ethnopharmacol. **212**, 188 (2018)
30. N. Arslan Burnaz, MSc Dissertation, *Karadeniz Technical University,* (2007).
31. O. Sagdic, A. Aksoy, G. Ozkan, Acta Aliment. **35**, 487 (2006)
32. D. Kajszczak, M. Zaklos-Szyda, A. Podsedek, Nutrients **12**, 1 (2020)
33. D. Polka, A. Podsedek, M. Koziołkiewicz, Plant Foods Hum. Nutr. **74**, 436 (2019)
34. M. Zaklos-Szyda, N. Pawlik, D. Polka, A. Nowak, M. Koziolkiewicz, A. Podsedek, Antioxidants **8**, 8 (2019)
35. I.A. Isoglu, N. Koc, Fibers Poly. **21**, 1453 (2020)
36. A. Yuruk-Durukan, I.A. Isoglu, Mater. Tech. **35**, 853 (2020)
37. N.N. Aksit, S. Gurdap, S.D. Isoglu, I.A. Isoglu, Int. J. Poly. Mat. Poly. Biomat. **70**, 797 (2021)
38. F.C. Bayram, M.F. Kapçı, A. Yuruk, I.A. Isoglu, B. Bal, Proc. Inst. Mech. Eng. E: J. Proces. Mech. Eng. **235**, 1957 (2021)
39. B. Sahin, A.S. Bulbul, I.S. Celik, N. Korkmaz, A. Karadag, Turk. J. Chem. **46**, 224 (2022)
40. B. Moldovan, L. David, A. Vulcu, L. Olenic, M. Perde-Schrepler, E. Fischer-Fodor, I. Baldea, S. Clichici, G.A. Filip, Mater. Sci. Eng. C **79**, 720 (2017)
41. I. Jahan, PhD Dissertation, Yıldız Tech. Uni. Grad. Sch. of Nat. and App. Sci. İstanbul, Turkey, 2019.
42. L. Ghasemi-Mobarakeh, M.P. Prabhakaran, M. Morshed, M.H. Nasr-Esfahani, S. Ramakrishna, Biomaterials **29**, 4532 (2008)
43. C.S. Ki, D.H. Baek, K.D. Gang, K.H. Lee, I.C. Um, Y.H. Park, Polymer **46**, 5094 (2005)
44. A. Jafari, A. Amirsadeghi, S. Hassanajili, N. Azarpira, Inter. J. Pharma. **583**, 119413 (2020)
45. E.M. Canga, F.C. Dudak, LWT-Food Sci. Tech. **110**, 247 (2019)
46. E.J. Chong, T.T. Phan, I.J. Lim, Y.Z. Zhang, B.H. Bay, S. Ramakrishna, C.T. Lim, Acta Biomater. **3**, 321 (2007)
47. X. Zhang, C. Chi, J. Chen, X. Zhang, M. Gong, X. Wang, J. Yan, R. Shi, L. Zhang, J. Xue, Mater. Des. **206**, 109732 (2021)
48. Z. Zhang, Q. Dai, Y. Zhang, H. Zhuang, E. Wang, Q. Xu, L. Ma, C. Wu, Z. Huan, F. Guo, J. Chang, A.C.S. Appl, Mater. Interfaces. **12**, 12489 (2020)
49. T. Amna, N.A. Barakat, M.S. Hassan, M.S. Khil, H.Y. Kim, Colloids Surf. A Physicochem Eng Asp **431**, 1 (2013)
50. F. Khan, M. Aldhahri, M.A. Hussain, K. Gauthaman, A. Memic, A. Abuzenadah, A. Kumosani, T. Barbour, E. Alothmany, R.W. Aldhaheri, J. Biomed. Nanotechnol. **14**, 553 (2018)
51. S. Suganya, T. Senthil-Ram, B.S. Lakshmi, V.R. Giridev, J. Appl. Polym. Sci. **121**, 2893 (2011)
52. A. Balaji, S.K. Jaganathan, A.F. Ismail, R. Rajasekar, Int J Nanomed. **11**, 4339 (2016)
53. S. Krainer, U. Hirn, Colloids Surf. A Physicochem. **619**, 126503 (2021)
54. L. Wang, J. Yang, X. Yang, Q. Hou, S. Liu, W. Zheng, Y. Long, X. Jiang, A.C.S. Appl, Mater. Interfaces. **12**, 51148 (2020)
55. M.E. Cam, S. Yildiz, H. Alenezi, S. Cesur, G.S. Ozcan, G. Erdemir, U. Edirisinghe, D. Anakin, D.S. Kuruca, L. Kabasakal, O. Gunduz, M. Edirisinghe, J.R. Soc, Interface **17**, 20190712 (2020)
56. Z. Hadisi, J. Nourmohammadi, S.M. Nassiri, Int. J. Biol. Macromol. **107**, 2008 (2018)
57. L. Si, C. Mengxia, J. Huayue, F. Linpeng, S. Binbin, Y. Fan, Y. Xingxing, L. Xiangxin, H. Chuanglong, W. Hongsheng, Colloids Surf. B: Biointerfaces **139**, 156 (2015)
58. R. Sedghi, A. Shaabani, Polymer **101**, 151 (2016)
59. W. Zhang, S. Ronca, E. Mele, Nanomaterials **7**, 42 (2017)
60. P.R. Cortez-Tornello, G.E. Feresin, A. Tapia, I.G. Veiga, Â.M. Moraes, G.A. Abraham, T.R. Cuadrado, Polym. J **44**, 1105 (2012)
61. S. Özbilgin, B. Ergene, M.L. Altun, B. Sever-Yılmaz, G. Saltan, E. Yuksel, Turk J Pharm Sci. **12**, 130 (2015)
62. M.P. Patil, Y. Seong, M.J. Kang, A.A. Singh, I. Niyonizigiye, G.D. Kim, J.K. Lee, J. Life Sci. **29**, 671 (2019)
63. M. Miklasińska-Majdanik, M. Kępa, R.D. Wojtyczka, D. Idzik, T.J. Wąsik, Int. J. Environ. Res. Public Health. **15**, 2321 (2018)
64. L. Cesoniene, R. Daubaras, V. Kraujalyte, P.R. Venskutonis, A. Sarkinas, J. fur Verbraucherschutz und Lebensmittelsicherheit **9**, 129 (2014)
65. Y.S. Velioglu, L. Ekici, E.S. Poyrazoglu, J. Food Sci. Techol. **44**, 252 (2006)
66. N. Unusan, J. Funct. Foods **67**, 103861 (2020)
67. M. Heidari, H. Bahrami, M. Ranjbar-Mohammadi, Mater. Sci. Eng. C **78**, 218 (2017)
68. M. Hadizadeh, M. Naeimi, M. Rafienia, A. Karkhaneh, Mater. Sci. Eng. C. **129**, 112362 (2021)
69. Z.P. Rad, J. Mokhtari, M. Abbasi, Iran. Polym. J. **28**, 51 (2019)
70. Z.P. Rad, J. Mokhtari, M. Abbasi, J. Biol. Macromol. **135**, 530 (2019)
71. A.G. Namboodiri, R. Parameswaran, Appl. Polym. Sci. **129**, 2280 (2013)

72. I.A. Isoglu, B. Bal, I.B. Tugluca, N. Koc, Mater. Res. Express **6**, 065411 (2019)
73. X. An, S. Duan, Z. Jiang, S. Chen, W. Sun, X. Liu, Z. Sun, Y. Li, M. Yan, Polym. Degrad. Stab. **206**, 110177 (2022)
74. D. Polka, A. Podsędekand, M. Koziołkiewicz, Plant Foods Hum. Nutr. **74**, 436 (2019)
75. M.L. Altun, G. Saltan-Çitoglu, B. Sever-Yilmaz, T. Coban, J. Food Sci. Nutr. **59**, 175 (2008)
76. B.I. Tarnowski, F.G. Spinale, J.H. Nicholson, Biotech Histochem **66**, 296 (1991)
77. M. Salehi, F. Bastami, Regen. Reconstr. Restor (Triple R) **1**, 69 (2016)
78. C.A. Bashur, L.A. Dahlgren, A.S. Goldstein, Biomaterials **27**, 5681 (2006)
79. C.H. Kim, M.S. Khil, H.Y. Kim, H.U. Lee, K.Y. Jahng, J. Biomed. Mater. Res. Part B Appl. Biomater. **78**, 283 (2006)
80. H. Matsumoto, A. Tanioka, Membranes **1**, 249 (2011)
81. F. Abedi, S.V. Moghaddam, P. Ghandforoushan, M. Aghazadeh, H. Ebadi, S. Davaran, J. Biol. Eng **16**, 1 (2022)
82. L.A. Can-Herrera, A.I. Oliva, M.A.A. Dzul-Cervantes, O.F. Pacheco-Salazar, J.M. Cervantes-Uc, Polymers **13**, 662 (2021)
83. Y. Wei, L. Gao, L. Wang, L. Shi, E. Wei, B. Zhou, L. Zhou, B. Ge, J. Drug Deliv. **24**, 681 (2017)
84. F.H. Fernandes, C.P. Santana, R.L. Santos, L.P. Correia, M.M. Conceição, R.O. Macêdo, A.C.D. Medeiros, J. Therm. Anal. Calorim **113**, 443 (2013)
85. M. Doostmohammadi, H. Forootanfar, M. Shakibaie, M. Torkzadeh-Mahani, H.R. Rahimi, E. Jafari, A. Ameri, A. Ameri, IET nanobiotechnol **15**, 277 (2021)
86. R.S. Costa, C.A.B. Negrão, S.R.P. Camelo, R.M. Ribeiro-Costa, W.L.R. Barbosa, C.E.F. Costa, J.O.C. Silva, J. Therm. Anal. Calorim **111**, 1959 (2013)
87. R. Barbosa, A. Villarreal, C. Rodriguez, H. De Leon, R. Gilkerson, K. Lozano, Mater. Sci. Eng. C **124**, 11206 (2021)